Marine Pollution Bulletin 142 (2019) 419–427

Contents lists available at ScienceDirect

Marine Pollution Bulletin

journal homepage: www.elsevier.com/locate/marpolbul

Indigenous PAH degraders along the gradient of the Yangtze Estuary of China: Relationships with pollutants and their bioremediation implications

Xinran Liu[a], Min Liu[a,b,*], Xing Chen[a], Yi Yang[a,c], Lijun Hou[c], Shixue Wu[a], Pinkuan Zhu[d]

[a] Key Laboratory of Geographic Information Science (Ministry of Education), School of Geographic Sciences, East China Normal University, Shanghai 200241, China
[b] Institute of Eco-Chongming (IEC), 3663 North Zhongshan Road, Shanghai 200062, China
[c] State Key Laboratory of Estuarine and Coastal Research, East China Normal University, 3663 North Zhongshan Road, Shanghai 200062, China
[d] School of Life Sciences, East China Normal University, Shanghai 200241, China

ARTICLE INFO

Keywords:
Microbial diversity
PAH degrader
Illumina MiSeq sequencing
Real-time quantitative PCR
Environmental gradient
Bioremediation

ABSTRACT

This study investigated the network of polycyclic aromatic hydrocarbon (PAH) degraders in the Yangtze estuarine and coastal areas. Along the estuarine gradients, Proteobacteria and Bacteroidetes were the dominant bacterial phyla, and forty-six potential PAH degraders were identified. The abundance of genes encoding the alpha subunit of the PAH-ring hydroxylating dioxygenases (PAH-RHDα) of gram-negative bacteria ranged from 5.5×10^5 to 5.8×10^7 copies g^{-1}, while that of gram-positive bacteria ranged from 1.3×10^5 to 2.0×10^7 copies g^{-1}. The PAH-degraders could represent up to 0.2% of the total bacterial community and mainly respond to PAHs and Cu concentrations, which indicate anthropogenic activities. Salinity and pH showed negative regulating effects on the PAH-degrading potential and the tolerance of bacteria to pollutants. PAH degraders such as *Novosphingobium* and *Mycobacterium* exhibit heavy-metal tolerance and core roles in the network of PAH degraders. These outcomes have important implications for bioremediation.

1. Introduction

Microorganisms in marine sediments play irreplaceable roles in pollutant transformation (Ribeiro et al., 2013), nutrient cycling (Bauer et al., 2013) and maintaining a healthy ecosystem (Besaury et al., 2013). The existence of natural environmental gradients (e.g., salinity and pH) in estuaries (Tremblay et al., 2005) makes them ideal niches for studying microbial responses to environmental factors, especially pollutants. Large amounts of pollutants enter estuaries through atmospheric deposition, urban storm waters and agricultural and industrial runoff (Duran and Cravo-Laureau, 2016; Lu et al., 2017). Microbial communities and functional bacteria can act as important biological indicators for these anthropogenic pollutants.

Among various pollutants, PAHs and heavy metals, representatives of organic and inorganic pollutants, respectively, are among the most harmful and often occur together in urban systems (Saeedi et al., 2012; Thavamani et al., 2012; Liu et al., 2017; Ma et al., 2017). The removal of PAHs pollution from environments is mainly achieved by microbial degradation. However, heavy metals may impair microbes by generating reactive oxygen species (ROS), destroying enzymatic activity, disrupting ion regulation and causing damage to DNA and protein compounds, which impacts the microbial degradation of PAHs (Gauthier et al., 2014), while PAHs can induce the generation of ROS and influence the microbial adsorption capability of heavy metals (Shen et al., 2006). In long-term contaminated soils with the co-occurrence of PAHs and heavy metals, Thavamani et al. (2012) found that microbial diversity was reduced and that enzyme activities were inhibited. Kuppusamy et al. (2016) observed dominant PAH degraders, including *Stenotrophomonas*, *Burkholderia* and *Pseudomonas*, and suggested harvesting indigenous heavy-metal tolerant PAH degraders from field-contaminated sites that may possess high degradation ability and tolerance to adverse conditions. However, studies on the indigenous PAH metabolic network of the microbial community and their relationships with organic and inorganic pollutants in long-term contaminated marine sediments remain scarce.

The main objectives of our study are (1) to explore the diversity and distribution of the microbial community, identify PAH degraders and estimate the PAH-degrading potential; (2) to characterize the environmental and pollutant gradients; and (3) to evaluate the impact of pollutants and environmental parameters on microbial communities and PAH degraders, as well as their implications for bioremediation in the densely populated Yangtze Estuary.

* Corresponding author at: Key Laboratory of Geographic Information Science (Ministry of Education), School of Geographic Sciences, East China Normal University, Shanghai 200241, China.
E-mail address: mliu@geo.ecnu.edu.cn (M. Liu).

https://doi.org/10.1016/j.marpolbul.2019.03.064
Received 25 November 2018; Received in revised form 21 March 2019; Accepted 31 March 2019
Available online 05 April 2019

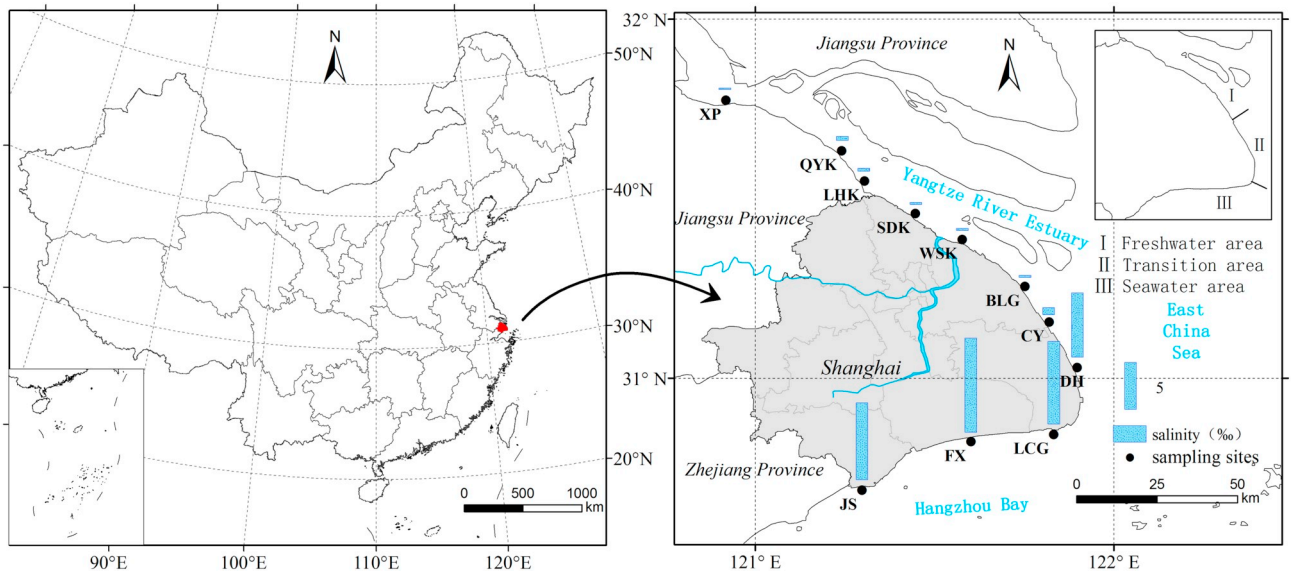

Fig. 1. Location and salinities of overlying waters for 11 sampling sites in the Yangtze Estuary and adjacent coastal areas of China. Section I includes XP, QYK, LHK, SDK, WSK and BLG, corresponds to low-salinity areas and is classified as freshwater areas; Section II includes CY and DH, corresponds to mid-salinity areas and is classified as transition areas; Section III includes LCG, FX and JS, corresponds to high-salinity areas and is classified as seawater areas.

2. Materials and methods

2.1. Sediment sampling

The Yangtze River belongs to the World's Top 10 Rivers at Risk by the World Wide Fund for Nature (Yin et al., 2015). The Yangtze Estuary accepts approximately 90% of terrestrial substances input into the East China Sea and is the main water source of metropolitan Shanghai (Yin et al., 2015). Surface sediments were collected using a stainless steel grab from the nearshore zone of the Yangtze estuarine and adjacent coastal areas. Eleven typical sampling locations were chosen based on the characteristics of the estuarine tidal ecosystem and historical research context (Xu et al., 1997). Sites XP, DH and BLG are located on the intertidal flat and are affected mainly by the Yangtze River and the East China Sea. QYK, LHK, WSK and CY, adjacent to the mouth of the urban river, are also influenced by urban river runoff. SDK is situated downstream from a wastewater treatment plant and is often affected by domestic sewage. LCG, FX and JS are located along the north bank of Hangzhou Bay and have strong hydrodynamic effects. Sampling was performed in October of 2015 and July of 2016 (Fig. 1). At each location, three 2 m^2 areas were chosen and surface sediment samples were collected in triplicate. Samples were put in sterile aluminum boxes, stored in an incubator box with ice, and transported to the laboratory within 8 h for immediate pretreatments and chemical analyses.

In the laboratory, each sediment sample was homogenized in an aseptic environment. Subsequently, one part of the homogeneous sample was stored at 4 °C for measurements of PAHs, heavy metals and physiochemical properties, while the other portion was stored at −80 °C for the immediate DNA extraction, 16S rRNA gene and PAH-degradation gene analysis. Based on the salinity gradients (Fig. 1), we classified the sampling locations as freshwater areas (XP, QYK, LHK, SDK, WSK and BLG), transition areas (CY and DH) and seawater areas (LCG, FX and JS).

2.2. Physicochemical properties

pH, total organic carbon (TOC), total nitrogen (TN), total phosphorus (TP) and grain size of sediments were analyzed using the methods from Li et al. (2015), the specification for marine monitoring (GB 17378.5–2007) (Administration of Quality Supervision, Inspection and Quarantine, 2008), Liu et al. (2014), Murphy and Riley (1962) and Dale et al. (2019), respectively. The procedures were detailed in the Supplementary information S1–2.2.

2.3. Characterization of microbial diversity and quantification of PAH-degrading genes

2.3.1. DNA extraction, PCR amplification and Illumina MiSeq sequencing

Genomic DNA was extracted in triplicate from surface sediment samples using the EZNA® Soil DNA Kit (Omega Bio-tek, Norcross, GA, U.S.). After mixing the triplicate DNA isolates together, the V3–V4 regions of the bacterial 16S ribosomal RNA gene were amplified using barcoded primers 338F (5′-ACTCCTACGGGAGGCAGCA-3′) and 806R (5′-GGACTACHVGGGTWTCTAAT-3′) by PCR (denaturation at 95 °C for 3 min, followed by 28 cycles at 95 °C for 30 s, 55 °C for 30 s, and 72 °C for 45 s, and a final extension at 72 °C for 10 min). PCR amplifications were conducted in triplicate 20 μL mixtures (4 μL of 5 × FastPfu Buffer, 2 μL of 2.5 mM dNTPs, 0.8 μL of each primer of 5 μM, 0.4 μL of FastPfu Polymerase and 10 ng of template DNA). Purified amplicons were pooled in equimolar concentrations and paired-end sequenced (2 × 300) or (2 × 250) on an Illumina MiSeq platform (Illumina, San Diego, USA) by Majorbio Bio-Pharm Technology Co. Ltd. (Shanghai, China). The raw reads were deposited into the NCBI Sequence Read Archive (SRA) database (Accession Number: SRP115975).

2.3.2. Real-time quantitative PCR

The real-time quantitative PCR (qPCR) was performed by the ABI 7500 Real-Time PCR system (Applied Biosystems, Canada). The abundance of total bacteria represented by the 16S rRNA gene was quantified using primers 341F (5′-CCTACGGGAGGCAGCAG-3′)/534R (5′-TTACCGCGGCTGCTGGCAC-3′) (Koike et al., 2007). The abundance of PAH degraders (PAH-RHDα gene) was quantified by primers for gram-positive (GP) PAH-$RHD_{[GP]}$ F (5′-CGGCGCCGACAAYTTYGTNGG-3′) and PAH-$PHD_{[GP]}$ R (5′-GGGGAACACGGTGCCRTGDATRAA-3′) and gram-negative (GN) PAH-$RHD_{[GN]}$ F (5′-GAGATGCATACCACGTKGGTTGGA-3′) and PAH-$RHD_{[GN]}$ R (5′-AGCTGTTGTTCGGGAAGAYWGTGCMGTT-3′) (Cebron et al., 2008). The procedures for PCR amplification, plasmid construction and qPCR are given in the Supplementary information (S1–2.3.2). The abundances of the 16S rRNA gene and PAH-RHDα gene were calculated separately based on their standard curves (Table S1).

2.3.3. Bioinformatic analyses

Raw fastq sequencing data were quality-filtered by Trimmomatic software (version 3.0) (Bolger et al., 2014) and merged by fast length adjustment of short reads (FLASH) software (version 1.2.7) (Magoc and Salzberg, 2011). Based on a threshold of 97% similarity, operational taxonomic units (OTUs) were clustered using UPARSE (version 7.1 http://drive5.com/uparse/). Chimeric sequences were detected and removed using UCHIME. The taxonomy of each 16S rRNA gene sequence was examined by the Ribosomal Database Project (RDP) Classifier algorithm (Wang et al., 2007) (http://rdp.cme.msu.edu/) against the Silva (SSU123) 16S rRNA database using a confidence threshold of 70%. Alpha-diversity indices, including community richness indices (Chao, Ace), community diversity indices (Shannon, Simpson), and the sequencing depth index (Good's coverage), were calculated using MOTHUR v.1.30.1 software (Schloss et al., 2011). A heatmap (Jami et al., 2013) reflecting the similarity and difference of the community composition of multiple samples at the taxonomic level of phylum and genus, respectively, was calculated using the vegan package and pheatmap package in R (Hou et al., 2016). To identify microbial lineages with significant differences between different groups of samples at various taxonomic levels, linear discriminate analysis (LDA) effect size (LEFSe) (Segata et al., 2011; Zhang et al., 2013) was applied. The significant abundance differences between two groups of PAH degraders were analyzed by the Welch's *t*-test (Ruxton, 2006). A rank-based nonparametric Kruskal-Wallis H test was used to determine if there are significant abundance differences among three groups of PAH degraders (Arboleya et al., 2016). Correlation heatmap analysis visually displays the obtained numerical matrix into the heatmap by calculating the Spearman's correlation between environmental factors and selected genera or other taxonomic levels (Yang et al., 2018). The co-occurrence and interaction patterns of PAH degraders were investigated through network analysis using Spearman's coefficient to indicate the relationship among bacteria (Rees et al., 2018). To identify the correlations between environmental factors and the microbial community, redundancy analysis (RDA) was performed using the R base vegan packages (Sheik et al., 2012). The significance of RDA analysis was determined by 999 Monte Carlo permutest analysis ($P < 0.05$). The length of an environmental parameter arrow in the RDA plot represents the strength of the correlation of that parameter to the community composition. The acute angle between an environmental parameter and a sample community indicates a positive relation between them, while the obtuse angle between a parameter and a community suggests a negative correlation between them (Wang et al., 2017).

2.4. Analysis of PAHs and heavy metals

The 16 USEPA priority PAHs (listed in the Supplement S1–2.4) were extracted from sediments using an accelerated solvent extractor (ASE350, Dionex, USA) and quantified by a gas chromatograph (7890A, Agilent, USA) coupled with a mass spectrometer (5977B, Agilent, USA). Spiked blanks (diatomite and pure copper powder, the supporting media of the extraction cells of the ASE) with 16 PAH standards were examined to assess the PAH losses during the experimental procedure, and the recoveries of 16 PAHs ranged from 72% to 106%. The PAH concentrations from two seasons were published in our previous study (Chen et al., 2018) while the analyses presented here were new. More details about PAH analysis procedures are given in our previous reports (Chen et al., 2018; Wu et al., 2018).

Sediment samples were digested in a graphite digestion instrument using a mixture of concentrated HCl-HNO_3-HF-$HClO_4$. Concentrations of Cr, Cu, Ni and Zn were measured by atomic absorption spectrometry (AA-6601F Model, Shimadzu Ltd., Japan), and Pb was measured using an ICP-MS (X-Series II Model, Thermo Fisher Scientific, USA). The concentrations of As and Hg were determined by atomic fluorescence spectrometry (AFS-930 Model, Haiguang, China) with an aqua regia digestion system from DB51/T 836-2008 of China. Blank tests, parallel tests, and standard recovery tests were applied to ensure quality control with relative deviations of parallel experiments less than ± 10%. Satisfactory recoveries were obtained for 95%–105%.

3. Results and discussion

3.1. The composition, diversity and distribution of the sedimentary microbial community and PAH degraders

After filtering out the low-quality reads, a total of 963,716 quality sequences from 22 samples from two seasons were retained. The sequence lengths were in the range of 279–541 bp, with a mean of 441 bp. In total, 6553 OTUs were identified, with 298 OTUs on average per sample. The OTU- and Shannon index-based rarefaction curves (Figs. S3 and S4) indicated that the depths of sequencing for bacteria were suitable for evaluating microbial diversity. As shown in Table S6, Good's coverage estimations revealed that 94% to 97% of the species were covered by sequencing in all samples. Ace, Chao, Shannon and Simpson indices showed that bacteria at 10CY had the highest biodiversity, while bacteria at 7SDK had the lowest diversity.

3.1.1. Taxonomic composition

The 6553 OTUs belong to 53 phyla, 132 classes and 959 genera. At different taxonomic levels, the 22 samples showed dissimilar 16S rRNA profiles (Fig. 2, Fig. S5). The dominant bacterial phyla of all samples were Proteobacteria, Bacteroidetes, Chloroflexi, Acidobacteria, Firmicutes and Nitrospirae. These six phyla in sum accounted for ~76% to 91% of the reads. Nitrospirae bacteria were not found to be significantly correlated with concentrations of chemical pollutants (e.g., PAHs) in estuarine sediments in a previous study (Lu et al., 2017). The abundances of Proteobacteria, Bacteroidetes, Firmicutes, Acidobacteria and Chloroflexi were also found in soils with long-term contamination by PAHs and heavy metals (Kuppusamy et al., 2016).

Based on the genes of PAH-RHDα and the reported PAHs degraders in the literature (Haritash and Kaushik, 2009; Kuppusamy et al., 2016; Liu et al., 2017; Lee et al., 2018), forty-six genera with potential PAH-

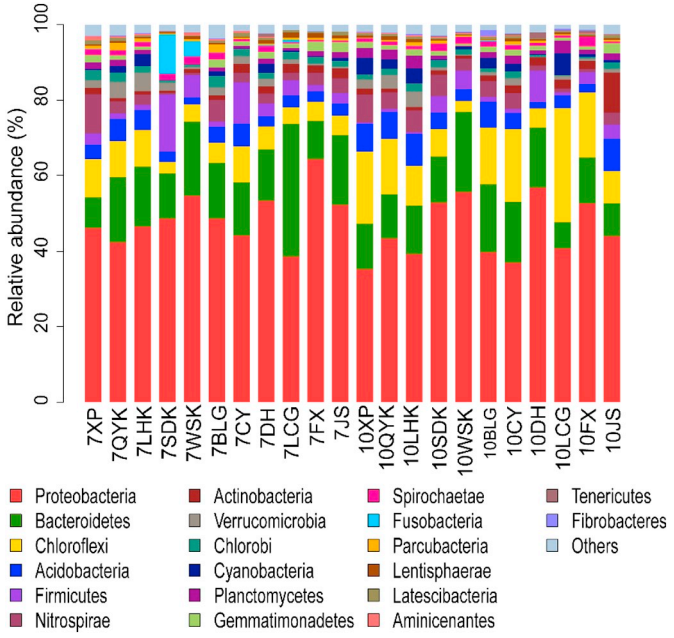

Fig. 2. Bacterial community structure of 22 sediment samples from the Yangtze Estuary showing the relative abundance of different phyla within each sample. Phyla with relative abundances below 1% were combined and indicated as others. Samples from July are indicated by the prefix "7", while samples from October are represented by the prefix "10".

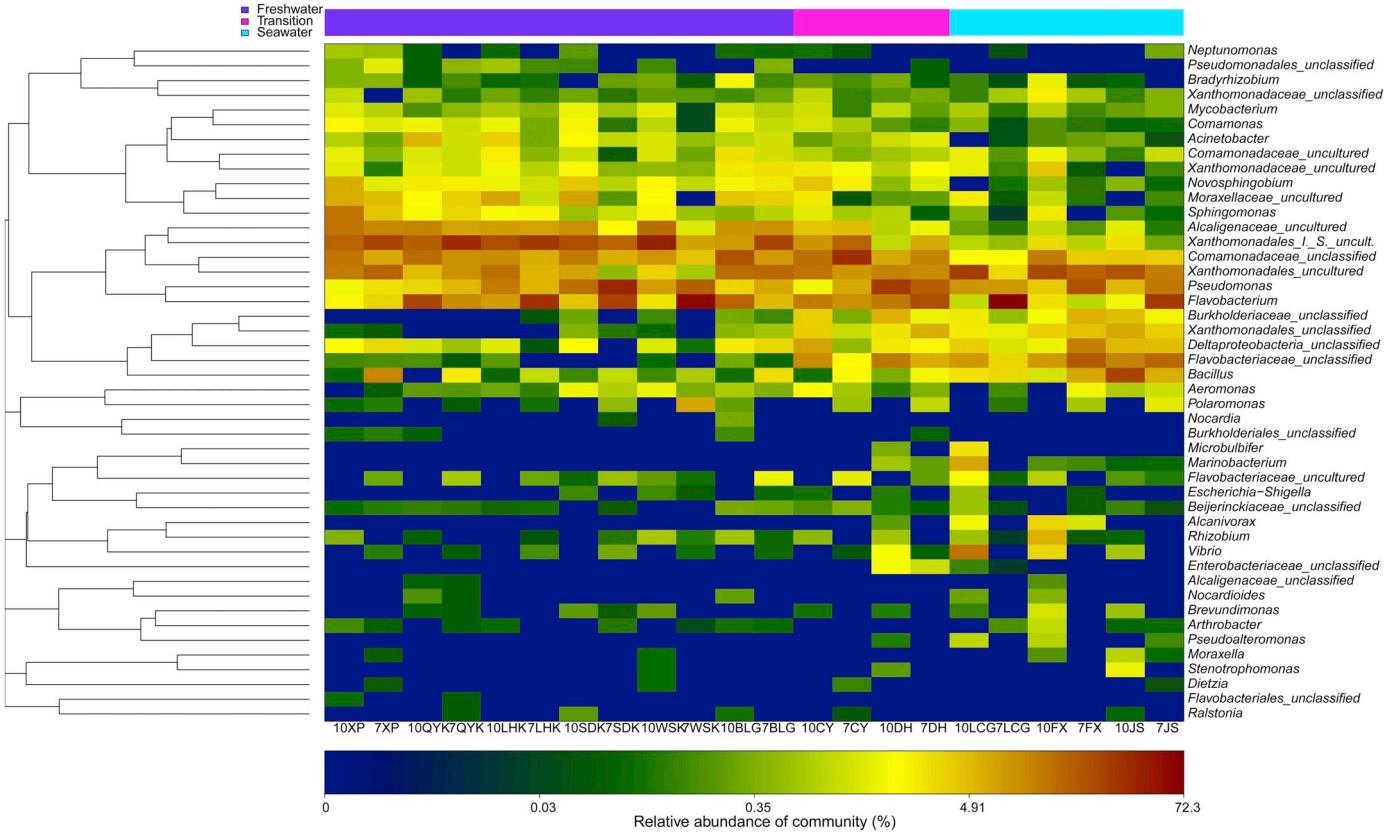

Fig. 3. Heatmap of 46 potential PAH degraders at the genus level in sediment samples of the Yangtze Estuary. The color scale at the bottom represents the relative abundance of one bacterial genus in the bacterial community of each sample. The color bar at the top represents three groups of samples: freshwater areas (10XP, 7XP, 10QYK, 7QYK, 10LHK, 7LHK, 10SDK, 7SDK, 10WSK, 7WSK, 10BLG, and 7BLG), transition areas (10CY, 7CY, 10DH and 7DH) and seawater areas (10LCG, 7LCG, 10FX, 7FX, 10JS and 7JS). The right side shows the genus name of each degrader while the left side exhibits their clustering results. Xanthomonadales_I._S._uncult. is the abbreviation of Xanthomonadales_Incertae_ Sedis_uncultured. (For interpretation of the references to color in this figure legend, the reader is referred to the web version of this article.)

degrading capability were identified in the investigated area; they are shown in the heatmap (Fig. 3). It reveals that the main degraders include Comamonadaceae_unclassified, *Pseudomonas*, *Flavobacterium*, Xanthomonadales_uncultured, Alcaligenaceae_uncultured, and *Bacillus*. It has been reported before that *Bacillus*, *Pseudomonas*, *Escherichia*, *Mycobacterium*, and *Enterobacter* are important bacteria for remediating cocontaminants of PAHs and heavy metals, indicating that they play a key bioremediating role in the PAH and heavy-metal copolluted Yangtze Estuary (Liu et al., 2017).

3.1.2. Temporospatial variation of microbiota and PAH degraders

The temporospatial abundance variation of the total microbial community was analyzed by LEFSe, and it is shown in the Supplementary information (Supplementary Fig. S8).

The seasonal abundance variation of PAH degraders was analyzed by Welch's *t*-test (Fig. 4A). Among the 15 most abundant degraders, *Flavobacterium* (GN) and *Polaromonas* (GN) were found to be significantly more abundant in July than in October. *Mycobacterium* (acid-fast organisms) showed a significantly higher abundance in October than in July. Fig. 5 shows the gene copy numbers of the 16S rRNA, PAH-RHDα GN and PAH-RHDα GP, the ratios of PAH-RHDα GN genes relative to 16S rRNA genes and the ratios of PAH-RHDα GP genes relative to 16S rRNA genes. The results revealed that the July samples contained more PAH-RHDα GN genes than in October. Therefore, LEFSe analysis for microbial community, Welch's *t*-test for PAH degraders and PAH-degrading gene analysis indicated that the July communities possessed higher PAH-degrading potential than those in October.

The spatial abundance variation of degraders (Fig. 4B) showed that *Bacillus* (GP), *Vibrio* (GN), *Marinobacterium* (GN) and *Alcanivorax* (GN) were significantly more abundant in seawater areas, while *Novosphingobium* (GN), *Sphingomonas* (GN), *Acinetobacter* (GN) and *Comamonas* (GN) were significantly more abundant in freshwater and transition areas. Moreover, the PAH-RHDα GN and GP gene analyses indicated that freshwater sediments contained a higher content of PAH-degrading genes than were found in transition and seawater areas (Fig. 5).

3.2. Abundances of PAH-degrading genes and bacterial genera tolerant to pollutants

As shown in Fig. 5 and Table S8, the abundances of the PAH-RHDα GN gene, the PAH-RHDα GP gene and the 16S rRNA gene were in the range of 5.5×10^5 to 5.8×10^7 copies g^{-1}, 1.3×10^5 to 2.0×10^7 copies g^{-1}, and 4.1×10^8 to 5.6×10^{10} copies g^{-1}, respectively. The lowest abundances of the 16S rRNA gene and the PAH-RHDα gene were observed in DH. The ratios of PAH-RHDα GN genes to 16S rRNA genes ranged from 0.009% to 0.215%, while the ratios of PAH-RHDα GP genes to 16S rRNA genes were in the range of 0.004% to 0.065%. The 16S rRNA gene copy number showed results comparable with our previous study (Guo et al., 2018). The abundance of PAH-RHDα genes was slightly lower than that in the urban roadside of Shanghai (Li et al., 2015), which was in the range of 5.7×10^6 to 6.44×10^7 copies g^{-1} in soil and slightly higher than that in soils and sediments of France, which ranged from 4.4×10^4 to 4.7×10^7 copies g^{-1} (Cebron et al., 2008).

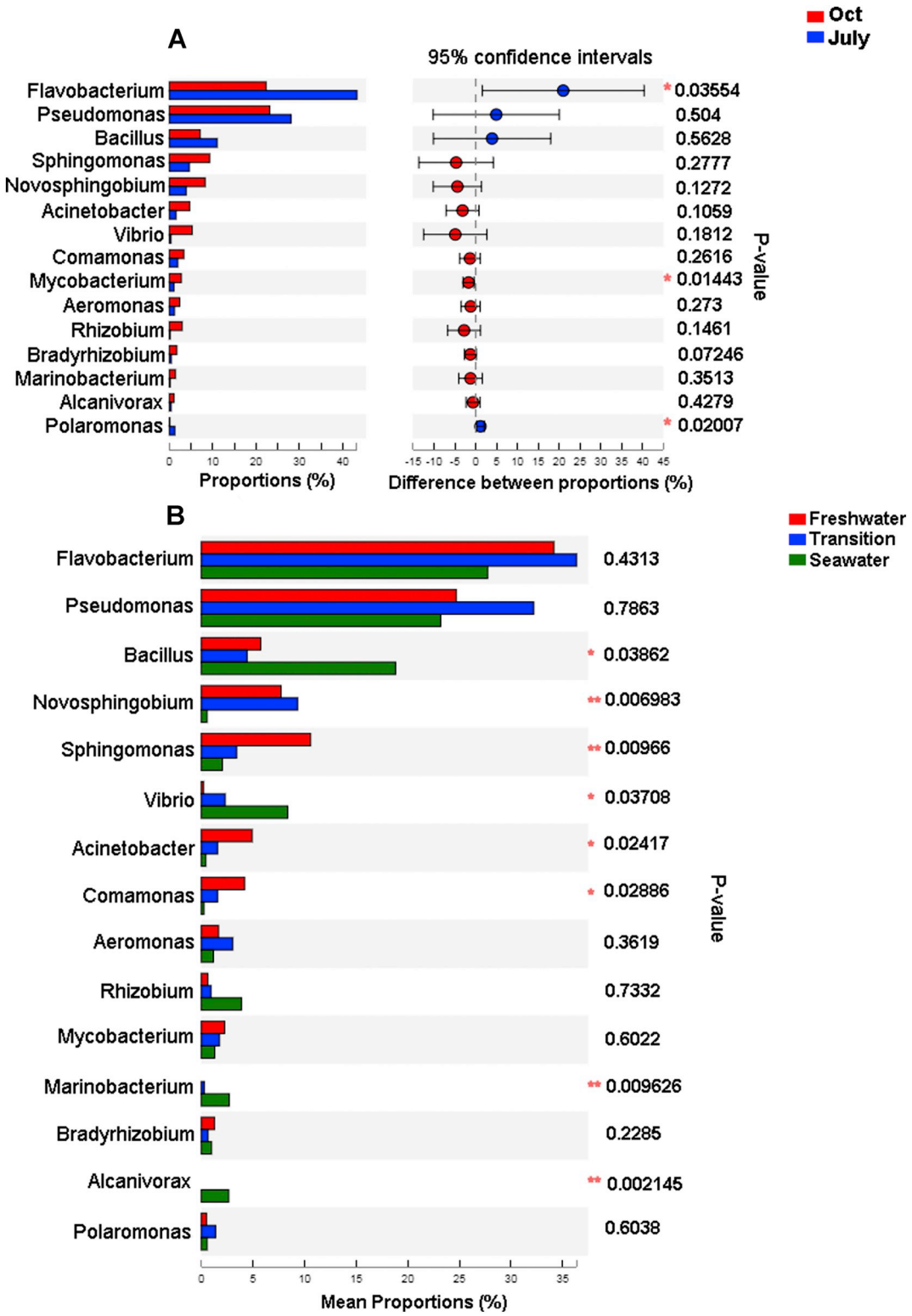

Fig. 4. Comparison of the differences in abundance of PAH degraders at the genus level in sediment samples from the Yangtze Estuary. (A) A comparison between communities from October and from July using Welch's *t*-test; (B) a comparison among communities from freshwater areas, transition areas and seawater areas using the Kruskal-Wallis H test.

As shown in the correlation heatmap in Fig. S10, among 46 PAH degraders, *Acinetobacter*, Xanthomonadales_Incertae_Sedis_uncultured, *Sphingomonas*, Alcaligenaceae_uncultured, Pseudomonadales_unclassified and Moraxellaceae_uncultured were positively correlated with PAHs, Zn, and Cu and even other heavy metals such as Pb, As, Ni. *Novosphingobium* and *Comamonas* showed positive correlations with PAHs and Hg. These PAH degraders tend to be heavy-metal tolerant and have important applications for bioremediation of PAHs in combined polluted areas. For example, *Sphingomonads* can transform heavy metals and utilize nutrients (Vilchez et al., 2007). *Mycobacterium* is known to degrade PAHs such as anthracene and benzo[*a*]pyrene and relieve the suppression given by heavy metals such as Cd, Cr and Pb coexisting with PAHs (Liu et al., 2017).

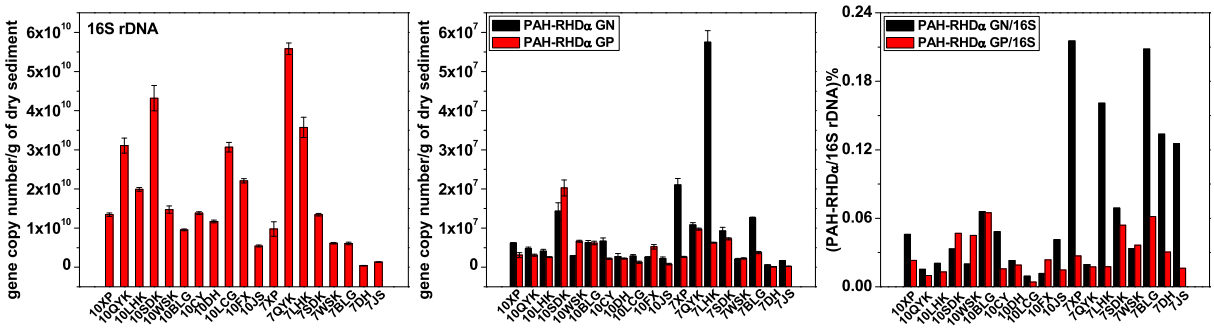

Fig. 5. The 16S rRNA, PAH-RHDα GN and GP gene copy numbers for the sediment samples from October and July from the Yangtze Estuary. Error bars represent standard errors of the three independent PCR runs. The ratios of PAH-RHDα GN and GP gene copy numbers to 16S rRNA gene copy numbers indicate the percentage of PAH degraders relative to the total bacterial community.

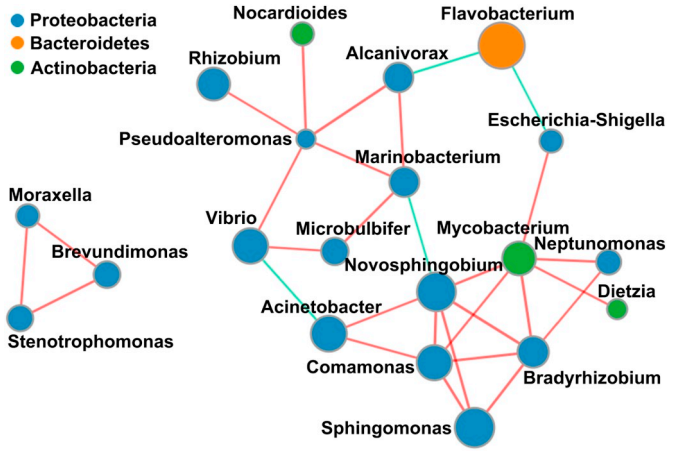

Fig. 6. Co-occurrence networks of dominant PAH degraders in the sediment samples from October and July from the 11 sampling sites of the Yangtze Estuary, showing their co-occurrence and coexclusion patterns. Red lines indicate positive correlations and green lines indicate negative correlations. The size of each node is proportional to the relative abundance of the corresponding species. (For interpretation of the references to color in this figure legend, the reader is referred to the web version of this article.)

3.3. Network analysis of the PAH degraders

The correlation network of PAH degraders (Fig. 6) revealed that the most correlating degraders were *Novosphingobium*, *Mycobacterium*, *Comamonas*, *Bradyrhizobium* and *Pseudoalteromonas*, implying that they are syntrophic bacteria and play central roles in the degradation of PAHs. The lower-correlating degraders were *Nocardioides*, *Rhizobium* and *Dietzia*. *Comamonas*, *Bradyrhizobium*, *Novosphingobium*, *Sphingomonas*, *Neptunomonas*, *Mycobacterium*, *Acinetobacter*, *Escherichia-Shigella* and *Dietzia* were correlated as a group, indicating that they may cooperate in their metabolic activities, e.g., PAH degradation. *Pseudoalteromonas*, *Alcanivorax*, *Vibrio*, *Marinobacterium*, *Nocardioides*, *Rhizobium* and *Microbulbifer* were connected as another group and showed coexclusion with the *Comamonas* group. This may be because degraders of this group primarily live in high-salinity areas and have functional connections during their life cycles. *Moraxella*, *Brevundimonas* and *Stenotrophomonas* were correlated with each other and had no linkage with other degraders, indicating that they may form another cooperative group during the metabolic process of pollutants. Previous studies found that PAH degraders widely cooperate while metabolizing PAHs, e.g., during the process of degradation of fluoranthene by a microbial community: *Mycobacterium* played a critical role in the initial degradation steps by generating the ring hydroxylating and ring cleavage dioxygenases; *Diaphorobacter* produced most of the dehydrogenases; *Hyphomicrobium*, *Agrobacterium*, and *Sphingopyxis* expressed enzymes catalyzing the downstream degradation (Zhao et al., 2016). The study of the bacterial correlations will provide a better understanding of the cooperative metabolic mechanisms of PAHs at a community level and thus help to improve the efficiency of bioremediation.

3.4. Pollution gradients of PAHs and heavy metals

Supplementary Fig. S1 and Table S3 show the total concentrations and compositions of 16 PAHs (TPAHs) at each sampling site. Seasonally, the TPAH concentrations of most sites were higher in July than in October (apart from FX, Fig. S1). Spatially, the TPAH concentrations in sediments varied in a pattern as freshwater area (F) > transition area (T) > seawater area (S) for both seasons. The trend is similar to that over four seasons shown in our previous study (Chen et al., 2018). The highest TPAH concentrations were in LHK, SDK and WSK, which was attributed to the high intensity of anthropogenic activities, receiving more urban river runoff, and being near effluent discharge outlets (Liu et al., 2004; Ou et al., 2010; Liu et al., 2012; Chen et al., 2018). Most individual components obeyed the same distribution pattern as the TPAHs. Minor exceptions included the concentrations of BbF, BaP and BghiP, which were especially high in FX in the seawater area in October and Ant in the transition areas (namely, CY and DH) in July.

Fig. S2 and Table S5 reveal the concentration ranges and mean contents (mg kg^{-1} d.w.) for seven heavy metals in surface sediments. Heavy-metal content was higher in July than in October except for Zn. The spatial distribution of Cr, Ni, Pb, Hg and As concentrations exhibited a pattern as transition areas > freshwater areas > seawater areas. However, Cu and Zn concentrations showed a decreasing trend as freshwater areas > transition areas > seawater areas.

The pollution-level comparisons of PAHs and heavy metals with other areas in the world are detailed in the Supplementary information (S2–3.4).

3.5. Relationships between the microbial community, PAH degraders, and gradients of PAH and heavy-metal residues

Fig. 7A shows the relationship between the total bacterial community and all 14 measured environmental parameters. Nine environmental factors showed a significant correlation with the community, namely, TP contents, salinity, TPAHs, Cu, Cr, Pb, TOC, Ni, and pH values. TP and salinity were the most important environmental parameters for explaining the distribution and structure of the bacterial communities, followed by TPAH concentrations and Cu contents. The significant correlation of TOC with the bacterial community corresponds to the fact that organic carbon is needed for shaping the microbial community structure and biogeographic distributions (Jorgensen et al., 2012; J. Liu et al., 2015). Salinity and geographic differences (namely, latitude and longitude) were reported to influence

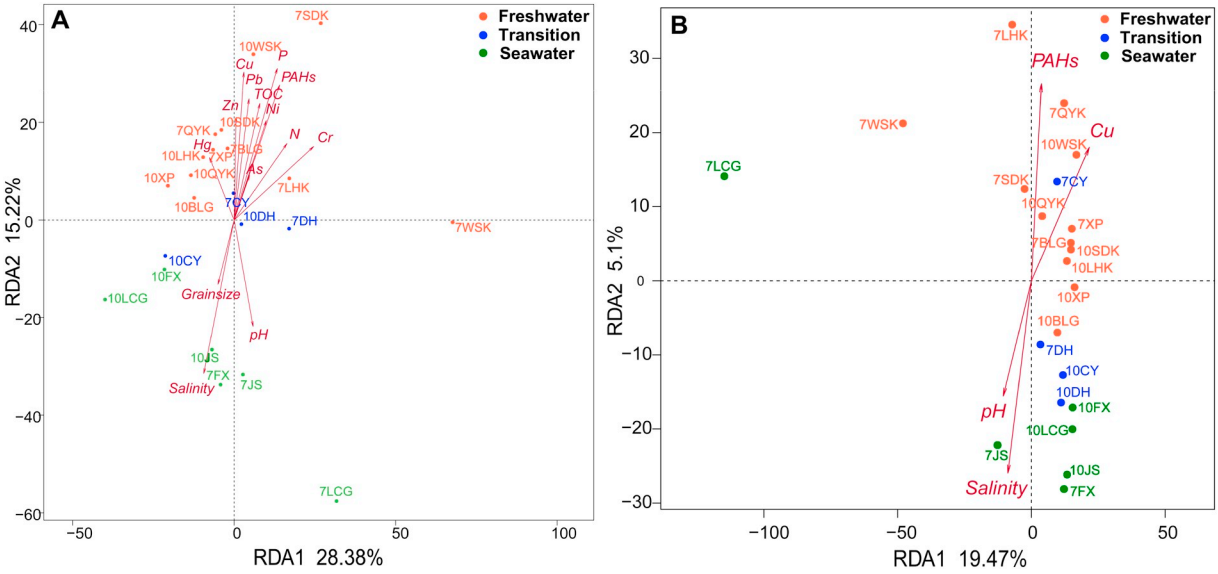

Fig. 7. Redundancy analysis (RDA) ordination plots showing the relationships between environmental parameters and bacterial communities (A) as well as PAHs degraders (B) in sediment samples from October and July from the Yangtze Estuary. Arrows represent the direction and magnitude of measured environmental factors associated with the bacterial communities. Color-coded dots along with site names represent the total bacterial communities or PAH degraders in each sample of different salinity groups. For the communities of all bacteria (A), fourteen environmental factors were analyzed, and nine factors showed significant correlation with the distribution and structure of the bacterial communities, namely, total P, salinity, PAHs, Cu, Cr, Pb, TOC, Ni and pH values. For the communities of PAH degraders (B), among 14 parameters analyzed, salinity, PAH contents, Cu concentrations and pH values significantly impacted the community of PAH degraders and were plotted. Each figure shows the first two principle dimensions, and all canonical axes were significant ($P < 0.05$). (For interpretation of the references to color in this figure legend, the reader is referred to the web version of this article.)

the microbial compositions (Lozupone and Knight, 2007; Liu et al., 2014). Heavy metals, independent of other contaminants, were a major regulator of bacterial community compositions (Kuppusamy et al., 2016). Moreover, the environmental pollutants TP, TPAHs, Cu, Pb, TOC and Ni showed a positive correlation with bacterial communities in freshwater areas (except for 7WSK), which had relatively low salinity and pH values, but showed a negative correlation with communities of seawater areas (plus 10CY of transition areas), which were of higher salinity and pH.

For PAH degraders (Fig. 7B), four significant impact factors were salinity, TPAH concentrations, Cu concentrations and pH values. Salinity was the most important environmental parameter impacting the structure of the PAH degrader communities. Again, pollutants TPAHs and Cu positively impacted degraders from most sites of freshwater areas (except 10XP and 10BLG) but negatively impacted those from transition areas (except 7CY) and seawater areas (except 7LCG).

Correlation heatmaps of 50 predominant genera from the total bacterial community (Supplementary Fig. S9) and of 46 PAH-degrader genera (Fig. S10) similarly reveal that bacteria growing in freshwater areas of lower salinity showed positive correlations with higher concentrations of TPAHs, P, Cu, Zn and some other pollutants. However, bacteria living primarily in higher salinity areas were mostly negatively correlated with the content of TPAHs, P, Cu, Zn and other pollutants. We thus inferred from RDA analyses and correlation heatmaps that the environmental salinity and pH values in this study negatively regulate the bioremediation ability and tolerance of bacteria to pollutants such as PAHs and heavy metals. It was reported previously that pH and salinity influenced the remediation efficiency of PAHs and heavy metals (Kastner et al., 1998; Thavamani et al., 2012; Liu et al., 2017). pH alters the toxicity of heavy metals to microbes by altering the valence states, redox potential, solubility and bioavailability of metals (Rodea-Palomares et al., 2009; Smith, 2009). The bioremediation efficiency of microbes is suppressed by acidic or alkaline pH values (Sandrin and Maier, 2002; Liu et al., 2017). It is a promising concept to promote the bioremediation of PAHs and heavy metals in contaminated areas by adjusting pH and salinity values.

The present study revealed that the abundance of PAH-RHDα genes of GN and GP had significant positive correlations with TPAH concentrations (Table S9), which was consistent with previous findings in soils and sediments (Cebron et al., 2008; Li et al., 2015). Salinity showed negative correlations with PAH degraders of GN and GP. Moreover, pH was negatively correlated and TP contents were positively correlated with GP PAH degraders, while Cu and Hg were positive controlling factors for GN PAH degraders. Therefore, the Spearman's correlation results of genes were consistent with that of RDA and the correlation heatmap analyses of bacteria. Two lines of evidence showed that the screening pressure exerted by PAH pollution would enrich populations capable of degrading PAHs in the environments. Salinity and pH have a negative impact on the PAH-degrading ability of bacteria, especially of GP degraders. Heavy metals such as Cu may enhance the PAH-degrading activity, especially of GN degraders.

3.6. Implications for bioremediation

The copollution of PAHs and heavy metals on the microbial ecology in estuarine areas is more complex than that for individual pollutants. The equilibrium between generation and removal of ROS within cells could be disturbed by stress factors such as salinity, heavy metals, PAHs and other pollutants, resulting in a sudden increase in ROS levels. ROS, including superoxide, hydrogen peroxide, hydroxyl radicals and their reaction products, can react nonspecifically and quickly with biomolecules, such as DNA, proteins, lipids and carbohydrates (Gill and Tuteja, 2010). Heavy-metal stress causes oxidation by ROS, which impairs enzymatic activity and DNA-protein compounds of microbes and influences the microbial degradation of PAHs (Gauthier et al., 2014). On the other hand, some heavy metals could induce microbial secretion of more proteins at low concentrations due to the excitatory effects of heavy metal poisons. These heavy metals can also act as cofactors for proteins to form enzyme-metal-substrate complexes, increasing the bioactivity of proteins and enhancing the enzymatic degradation of PAHs. For example, Pb(II) enhances Phe biodegradation at low concentrations but decreases Phe biodegradation at excessive

concentrations (S.-H. Liu et al., 2015). Studies have also shown that under conditions of PAH-heavy metal complex pollution, heavy metals, e.g., Cu(II), can stress the microbial secretion of new degrading enzymes and thus change the degradation pathway of PAHs (Chen et al., 2013).

PAHs can induce the generation of ROS that can exert oxidative stress on bacteria and influence the microbial adsorption capability of heavy metals. PAHs can exert a narcotic effect on the lipophilic compounds of microbial cells, which enables heavy metals to infiltrate into microbial cells more facilely and affect microbial functions (Shen et al., 2006). On the other hand, PAHs can alter the fluidity of the membranes and the electrical potential of cells, which inhibits the adsorption of heavy metals by microbes (Gorria et al., 2006). It is also anticipated that PAHs could disrupt the metal-ATPase activity, which would impact the transport of heavy metals (Gauthier et al., 2015). How bacteria accommodate the combined pollution of PAHs and heavy metals and detoxify these long-present pollutants remains to be further studied.

Microbes harvested from naturally polluted areas may possess higher degradation ability and higher tolerance to adverse conditions such as other pollutants (e.g., heavy metals), the deficiency of nutrients, and the adverse conditions of higher salinity and pH than microbes from spiked media (Kuppusamy et al., 2016) and could, therefore, better bioremediate real contaminated fields.

Conflicts of interest

There are no conflicts of interest to declare.

Acknowledgements

We thank the editor and anonymous reviewers for their expert comments and help. This work was supported by the National Natural Science Foundation of China [grant numbers 41501530, 41730646 and 41761144062]. We acknowledge Chong Wang and Xianbiao Lin for their help in figure drawing and Jing Yang for laboratory help.

Appendix A. Supplementary data

Supplementary data to this article can be found online at https://doi.org/10.1016/j.marpolbul.2019.03.064.

References

Administration of Quality Supervision, Inspection and Quarantine, 2008. The Specification for Marine Monitoring, Part 5: Sediment Analysis: GB 17378.5-2007. Standards Press of China, Beijing.

Arboleya, S., Sanchez, B., Solis, G., Fernandez, N., Suarez, M., Hernandez-Barranco, A.M., Milani, C., Margolles, A., de los Reyes-Gavilan, C.G., Ventura, M., Gueimonde, M., 2016. Impact of prematurity and perinatal antibiotics on the developing intestinal microbiota: a functional inference study. Int. J. Mol. Sci. 17.

Bauer, J.E., Cai, W.-J., Raymond, P.A., Bianchi, T.S., Hopkinson, C.S., Regnier, P.A.G., 2013. The changing carbon cycle of the coastal ocean. Nature 504, 61–70.

Besaury, L., Marty, F., Buquet, S., Mesnage, V., Muyzer, G., Quillet, L., 2013. Culture-dependent and independent studies of microbial diversity in highly copper-contaminated Chilean marine sediments. Microb. Ecol. 65, 311–324.

Bolger, A.M., Lohse, M., Usadel, B., 2014. Trimmomatic: a flexible trimmer for Illumina sequence data. Bioinformatics 30, 2114–2120.

Cebron, A., Norini, M.-P., Beguiristain, T., Leyval, C., 2008. Real-time PCR quantification of PAH-ring hydroxylating dioxygenase (PAH-RHD alpha) genes from Gram positive and Gram negative bacteria in soil and sediment samples. J. Microbiol. Methods 73, 148–159.

Chen, S., Yin, H., Ye, J., Peng, H., Zhang, N., He, B., 2013. Effect of copper(II) on biodegradation of benzo a pyrene by Stenotrophomonas maltophilia. Chemosphere 90, 1811–1820.

Chen, X., Liu, X., Liu, M., Yang, Y., Wu, S., Wang, C., 2018. Molecular characterization of PAHs based on land use analysis and multivariate source apportionment in multiple phases of the Yangtze estuary, China. Environ. Sci. Processes Impacts 20, 531–543.

Dale, J., Cundy, A.B., Spencer, K.L., Carr, S.J., Croudace, I.W., Burgess, H.M., Nash, D.J., 2019. Sediment structure and physicochemical changes following tidal inundation at a large open coast managed realignment site. Sci. Total Environ. 660, 1419–1432.

Duran, R., Cravo-Laureau, C., 2016. Role of environmental factors and microorganisms in determining the fate of polycyclic aromatic hydrocarbons in the marine environment. FEMS Microbiol. Rev. 40, 814–830.

Gauthier, P.T., Norwood, W.P., Prepas, E.E., Pyle, G.G., 2014. Metal-PAH mixtures in the aquatic environment: a review of co-toxic mechanisms leading to more-than-additive outcomes. Aquat. Toxicol. 154, 253–269.

Gauthier, P.T., Norwood, W.P., Prepas, E.E., Pyle, G.G., 2015. Metal-polycyclic aromatic hydrocarbon mixture toxicity in Hyalella azteca. 1. Response surfaces and isoboles to measure non-additive mixture toxicity and ecological risk. Environ. Sci. Technol. 49, 11772–11779.

Gill, S.S., Tuteja, N., 2010. Reactive oxygen species and antioxidant machinery in abiotic stress tolerance in crop plants. Plant Physiol. Biochem. 48, 909–930.

Gorria, M., Tekpli, X., Sergent, O., Huc, L., Gaboriau, F., Rissel, M., Chevanne, M., Dimanche-Boitrel, M.-T., Lagadic-Gossmann, D., 2006. Membrane fluidity changes are associated with benzo a pyrene-induced apoptosis in F258 cells - protection by exogenous cholesterol, in: Diederich, M. (Ed.), Signal Transduction Pathways, Pt A: Apoptotic and Extracellular Signaling, pp. 108–112.

Guo, X.-p., Lu, D.-p., Niu, Z.-s., Feng, J.-n., Chen, Y.-r., Tou, F.-y., Liu, M., Yang, Y., 2018. Bacterial community structure in response to environmental impacts in the intertidal sediments along the Yangtze Estuary, China. Mar. Pollut. Bull. 126, 141–149.

Haritash, A.K., Kaushik, C.P., 2009. Biodegradation aspects of Polycyclic Aromatic Hydrocarbons (PAHs): a review. J. Hazard. Mater. 169, 1–15.

Hou, Q., Kwok, L.-Y., Zheng, Y., Wang, L., Guo, Z., Zhang, J., Huang, W., Wang, Y., Leng, L., Li, H., Zhang, H., 2016. Differential fecal microbiota are retained in broiler chicken lines divergently selected for fatness traits. Sci. Rep. 6, 37376–37388.

Jami, E., Israel, A., Kotser, A., Mizrahi, I., 2013. Exploring the bovine rumen bacterial community from birth to adulthood. ISME J. 7, 1069–1079.

Jorgensen, S.L., Hannisdal, B., Lanzén, A., Baumberger, T., Flesland, K., Fonseca, R., Øvreås, L., Steen, I.H., Thorseth, I.H., Pedersen, R.B., Schleper, C., 2012. Correlating microbial community profiles with geochemical data in highly stratified sediments from the Arctic Mid-Ocean Ridge. Proc. Natl. Acad. Sci. 109, E2846–E2855.

Kastner, M., Breuer-Jammali, M., Mahro, B., 1998. Impact of inoculation protocols, salinity, and pH on the degradation of polycyclic aromatic hydrocarbons (PAHs) and survival of PAH-degrading bacteria introduced into soil. Appl. Environ. Microbiol. 64, 359–362.

Koike, S., Krapac, I.G., Oliver, H.D., Yannarell, A.C., Chee-Sanford, J.C., Aminov, R.I., Mackie, R.I., 2007. Monitoring and source tracking of tetracycline resistance genes in lagoons and groundwater adjacent to swine production facilities over a 3-year period. Appl. Environ. Microbiol. 73, 4813–4823.

Kuppusamy, S., Thavamani, P., Megharaj, M., Venkateswarlu, K., Lee, Y.B., Naidu, R., 2016. Pyrosequencing analysis of bacterial diversity in soils contaminated long-term with PAHs and heavy metals: implications to bioremediation. J. Hazard. Mater. 317, 169–179.

Lee, D.W., Lee, H., Lee, A.H., Kwon, B.-O., Khim, J.S., Yim, U.H., Kim, B.S., Kim, J.-J., 2018. Microbial community composition and PAHs removal potential of indigenous bacteria in oil contaminated sediment of Taean coast, Korea. Environ. Pollut. 234, 503–512.

Li, X., Hou, L., Liu, M., Zheng, Y., Li, Y., Lin, X., 2015. Abundance and diversity of polycyclic aromatic hydrocarbon degradation bacteria in urban roadside soils in Shanghai. Appl. Microbiol. Biotechnol. 99, 3639–3649.

Liu, M., Yang, Y., Xu, S., Hou, L., Liu, Q., Ou, D., Jiang, H., 2004. Persistent organic pollutants (POPS) in intertidal surface sediments from the Yangtze Estuarine and coastal areas, China. J. Coast. Res. 162–170.

Liu, L.-Y., Wang, J.-Z., Wei, G.-L., Guan, Y.-F., Zeng, E.Y., 2012. Polycyclic aromatic hydrocarbons (PAHs) in continental shelf sediment of China: implications for anthropogenic influences on coastal marine environment. Environ. Pollut. 167, 155–162.

Liu, J., Yang, H., Zhao, M., Zhang, X.-H., 2014. Spatial distribution patterns of benthic microbial communities along the Pearl Estuary, China. Syst. Appl. Microbiol. 37, 578–589.

Liu, J., Sui, Y., Yu, Z., Shi, Y., Chu, H., Jin, J., Liu, X., Wang, G., 2015a. Soil carbon content drives the biogeographical distribution of fungal communities in the black soil zone of northeast China. Soil Biol. Biochem. 83, 29–39.

Liu, S.-H., Zeng, G.-M., Niu, Q.-Y., Gong, J.-L., Hu, X.-J., Lu, L.-H., Zhou, Y.-Y., Hu, X., Chen, M., Yan, M., 2015b. Effect of Pb(II) on phenanthrene degradation by new isolated Bacillus sp P1. RSC Adv. 5, 55812–55818.

Liu, S.-H., Zeng, G.-M., Niu, Q.-Y., Liu, Y., Zhou, L., Jiang, L.-H., Tan, X.-f., Xu, P., Zhang, C., Cheng, M., 2017. Bioremediation mechanisms of combined pollution of PAHs and heavy metals by bacteria and fungi: a mini review. Bioresour. Technol. 224, 25–33.

Lozupone, C.A., Knight, R., 2007. Global patterns in bacterial diversity. Proc. Natl. Acad. Sci. 104, 11436–11440.

Lu, X.-M., Chen, C., Zheng, T.-L., 2017. Metagenomic insights into effects of chemical pollutants on microbial community composition and function in estuarine sediments receiving polluted river water. Microb. Ecol. 73, 791–800.

Ma, Y., Liu, A., Egodawatta, P., McGree, J., Goonetilleke, A., 2017. Assessment and management of human health risk from toxic metals and polycyclic aromatic hydrocarbons in urban stormwater arising from anthropogenic activities and traffic congestion. Sci. Total Environ. 579, 202–211.

Magoc, T., Salzberg, S.L., 2011. FLASH: fast length adjustment of short reads to improve genome assemblies. Bioinformatics 27, 2957–2963.

Murphy, J., Riley, J.P., 1962. A modified single solution method for the determination of phosphate in natural waters. Anal. Chim. Acta 27, 31–36.

Ou, D., Liu, M., Cheng, S., Hou, L., Xu, S., Wang, L., 2010. Identification of the sources of polycyclic aromatic hydrocarbons based on molecular and isotopic characterization from the Yangtze estuarine and nearby coastal areas. J. Geogr. Sci. 20, 283–294.

Rees, C.A., Burklund, A., Stefanuto, P.-H., Schwartzman, J.D., Hill, J.E., 2018. Comprehensive volatile metabolic fingerprinting of bacterial and fungal pathogen groups. J. Breath Res. 12.

Ribeiro, H., Mucha, A.P., Almeida, C.M.R., Bordalo, A.A., 2013. Bacterial community response to petroleum contamination and nutrient addition in sediments from a temperate salt marsh. Sci. Total Environ. 458, 568–576.
Rodea-Palomares, I., Gonzalez-Garcia, C., Leganes, F., Fernandez-Pinas, F., 2009. Effect of pH, EDTA, and anions on heavy metal toxicity toward a bioluminescent cyanobacterial bioreporter. Arch. Environ. Contam. Toxicol. 57, 477–487.
Ruxton, G.D., 2006. The unequal variance t-test is an underused alternative to Student's t-test and the Mann-Whitney U test. Behav. Ecol. 17, 688–690.
Saeedi, M., Li, L.Y., Salmanzadeh, M., 2012. Heavy metals and polycyclic aromatic hydrocarbons: pollution and ecological risk assessment in street dust of Tehran. J. Hazard. Mater. 227, 9–17.
Sandrin, T.R., Maier, R.M., 2002. Effect of pH on cadmium toxicity, speciation, and accumulation during naphthalene biodegradation. Environ. Toxicol. Chem. 21, 2075–2079.
Schloss, P.D., Gevers, D., Westcott, S.L., 2011. Reducing the effects of PCR amplification and sequencing artifacts on 16S rRNA-based studies. PLoS One 6.
Segata, N., Izard, J., Waldron, L., Gevers, D., Miropolsky, L., Garrett, W.S., Huttenhower, C., 2011. Metagenomic biomarker discovery and explanation. Genome Biol. 12, R60.
Sheik, C.S., Mitchell, T.W., Rizvi, F.Z., Rehman, Y., Faisal, M., Hasnain, S., McInerney, M.J., Krumholz, L.R., 2012. Exposure of soil microbial communities to chromium and arsenic alters their diversity and structure. PLoS One 7.
Shen, G.Q., Lu, Y.T., Hong, J.B., 2006. Combined effect of heavy metals and polycyclic aromatic hydrocarbons on urease activity in soil. Ecotoxicol. Environ. Saf. 63, 474–480.
Smith, S.R., 2009. A critical review of the bioavailability and impacts of heavy metals in municipal solid waste composts compared to sewage sludge. Environ. Int. 35, 142–156.
Thavamani, P., Malik, S., Beer, M., Megharaj, M., Naidu, R., 2012. Microbial activity and diversity in long-term mixed contaminated soils with respect to polyaromatic hydrocarbons and heavy metals. J. Environ. Manag. 99, 10–17.
Tremblay, L., Kohl, S.D., Rice, J.A., Gagne, J.P., 2005. Effects of temperature, salinity, and dissolved humic substances on the sorption of polycyclic aromatic hydrocarbons to estuarine particles. Mar. Chem. 96, 21–34.
Vilchez, R., Pozo, C., Gomez, M.A., Rodelas, B., Gonzalez-Lopez, J., 2007. Dominance of sphingomonads in a copper-exposed biofilm community for groundwater treatment. Microbiology 153, 325–337.
Wang, Q., Garrity, G.M., Tiedje, J.M., Cole, J.R., 2007. Naive Bayesian classifier for rapid assignment of rRNA sequences into the new bacterial taxonomy. Appl. Environ. Microbiol. 73, 5261–5267.
Wang, Y.Y., Chen, J., Zhou, S.A., Wang, X.D., Chen, Y., Lin, X.M., Yan, Y., Ma, X., Wu, M., Han, H.C., 2017. 16S rRNA gene high-throughput sequencing reveals shift in nitrogen conversion related microorganisms in a CANON system in response to salt stress. Chem. Eng. J. 317, 512–521.
Wu, S., Liu, X., Liu, M., Chen, X., Liu, S., Cheng, L., Lin, X., Li, Y., 2018. Sources, influencing factors and environmental indications of PAH pollution in urban soil columns of Shanghai, China. Ecol. Indic. 85, 1170–1180.
Xu, S.Y., Tao, J., Chen, Z.L., Chen, Z.Y., Lü, Q.R., 1997. Dynamic accumulation of heavy metals in tidal flat sediments of Shanghai. Oceanol. Limnol. Sin. 28, 509–515.
Yang, Y.D., Ren, Y.F., Wang, X.Q., Hu, Y.G., Wang, Z.M., Zeng, Z.H., 2018. Ammonia-oxidizing archaea and bacteria responding differently to fertilizer type and irrigation frequency as revealed by Illumina Miseq sequencing. J. Soils Sediments 18, 1029–1040.
Yin, S., Feng, C., Li, Y., Yin, L., Shen, Z., 2015. Heavy metal pollution in the surface water of the Yangtze Estuary: a 5-year follow-up study. Chemosphere 138, 718–725.
Zhang, C., Li, S., Yang, L., Huang, P., Li, W., Wang, S., Zhao, G., Zhang, M., Pang, X., Yan, Z., Liu, Y., Zhao, L., 2013. Structural modulation of gut microbiota in life-long calorie-restricted mice. Nat. Commun. 4.
Zhao, J.-K., Li, X.-M., Ai, G.-M., Deng, Y., Liu, S.-J., Jiang, C.-Y., 2016. Reconstruction of metabolic networks in a fluoranthene-degrading enrichments from polycyclic aromatic hydrocarbon polluted soil. J. Hazard. Mater. 318, 90–98.